Supplementary Information

Highly Dispersed Ni-Fe Active Sites on Fullerene based Electron Buffer to boost Oxygen Evolution Reaction

Qin Tang,[a] Lingyue Wang,[a] Shenglong Zhang,[a] Pengfei Xue,[b] Yuye Zhang,[a] Hongbo Li,[a]* Dongdong Zhu[b]*

[a.] School of Chemistry and Chemical Engineering, Yancheng Institute of Technology, Yancheng, 224051, China. Email: hbli@ycit.edu.cn

[b.] School of Chemistry and Materials Science, Institute of Advanced Materials and Flexible Electronics (IAMFE), Nanjing University of Information Science and Technology, 219 Ningliu Road, Nanjing, 210044, China. E-mail: dd.zhu@nuist.edu.cn

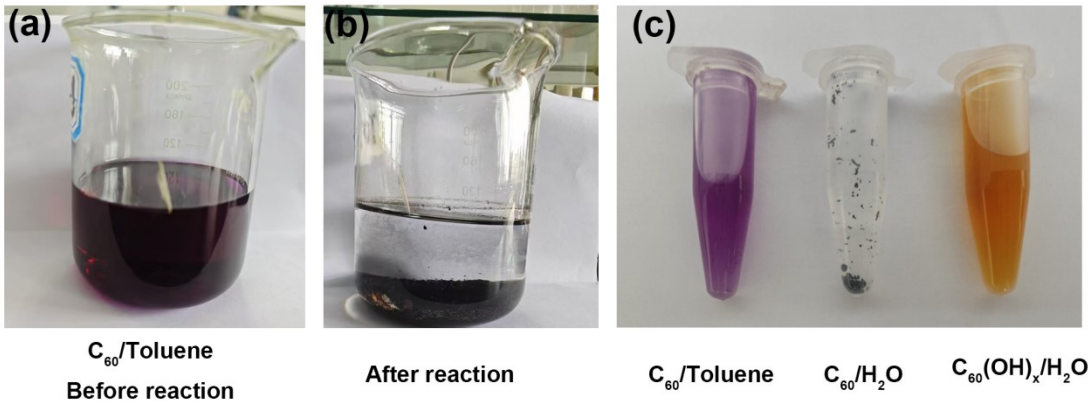

Fig. S1 Digital photos of C_{60} in toluene (a) before reaction, (b) after reaction, (c) contrast of C_{60} in toluene, C_{60} in H_2O and $C_{60}(OH)_x$ in H_2O.

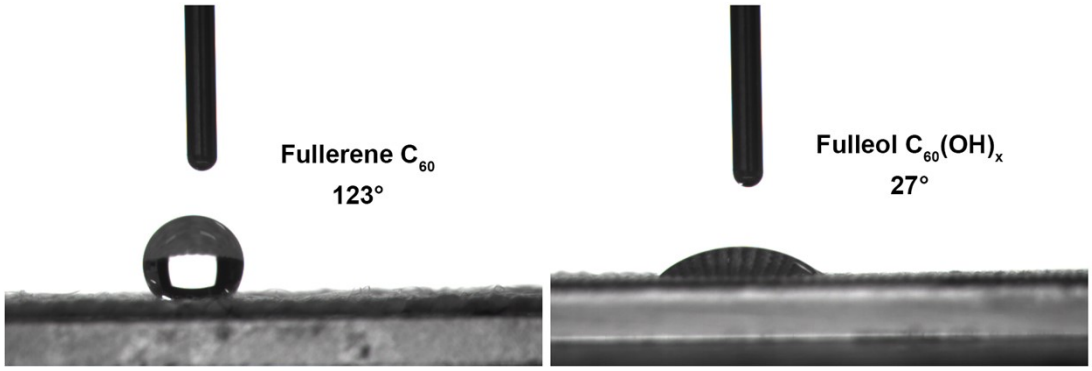

Fig. S2 Contact angles of fullerene C_{60} and fulleol $C_{60}(OH)_x$.

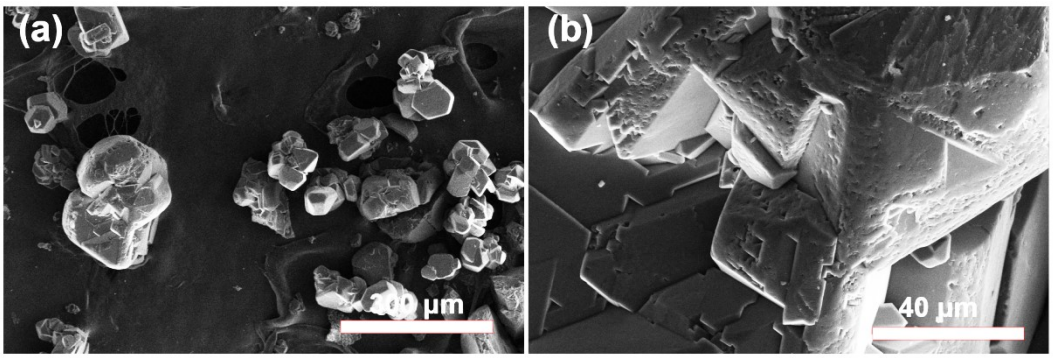

Fig. S3 (a-b) SEM images of C_{60} powders.

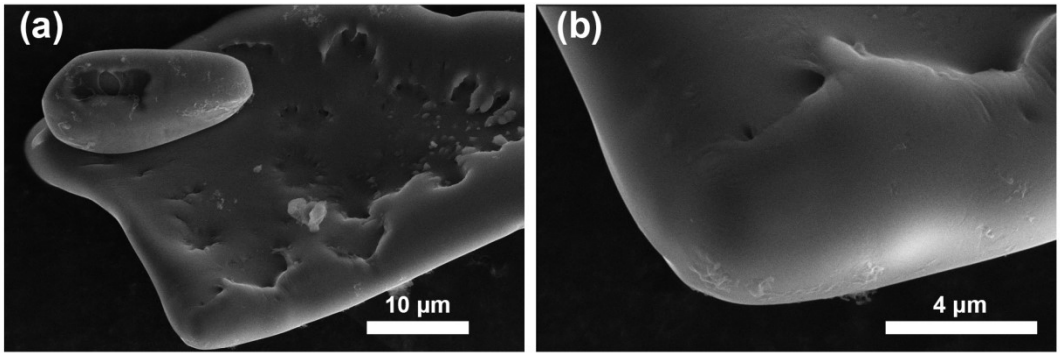

Fig. S4 (a-b) SEM images of $C_{60}(OH)_x$ powders.

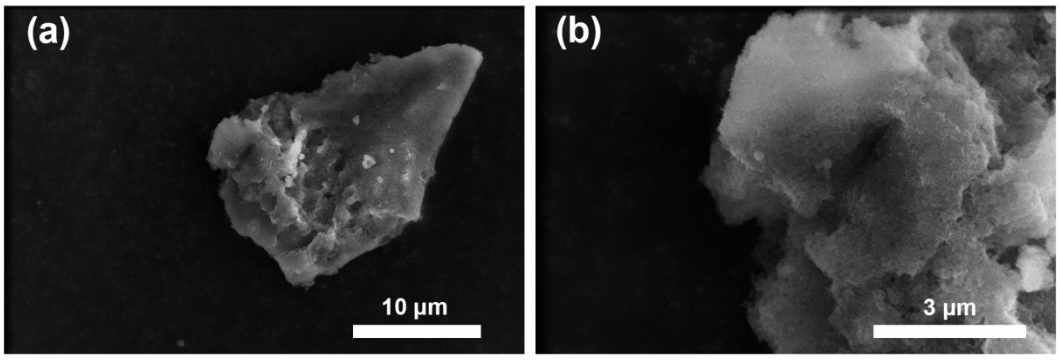

Fig. S5 (a-b) SEM images of NiFe-OC_{60} powders.

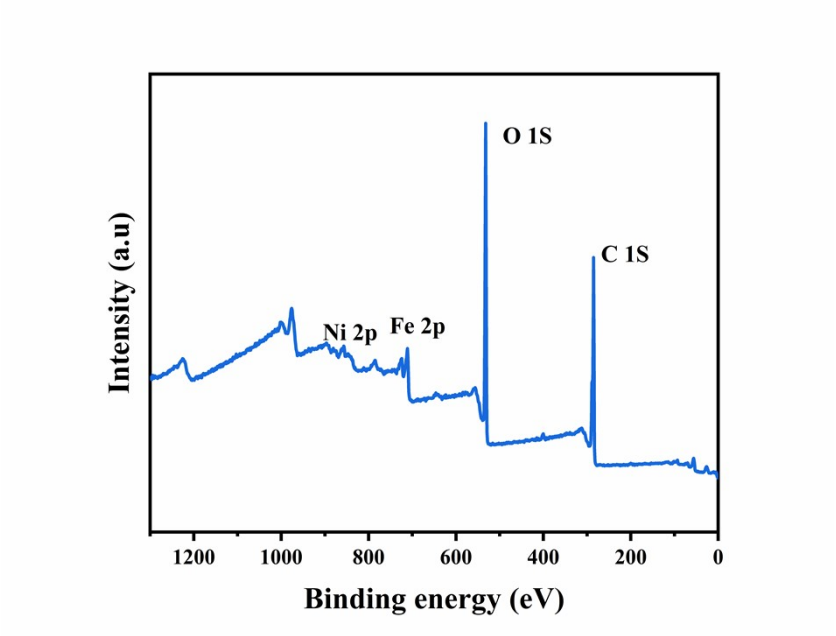

Fig. S6 XPS survey spectrum of NiFe-OC_{60}.

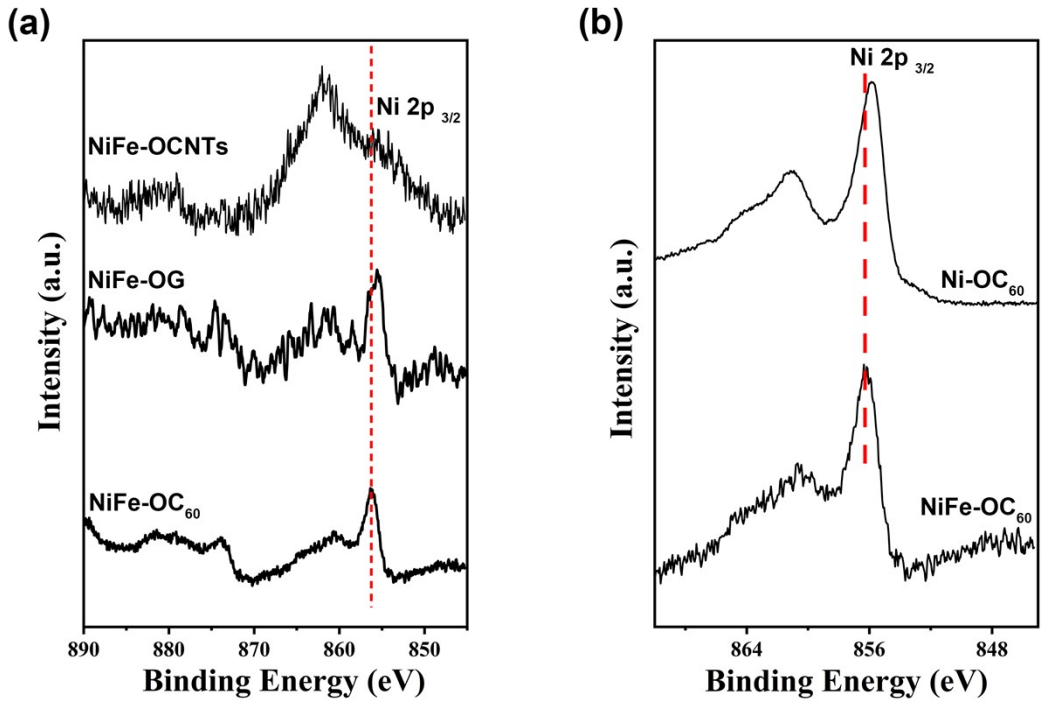

Fig. S7 (a) XPS Ni 2p spectra of NiFe-OCNTs, NiFe-OG and NiFe-OC_{60}, (b) XPS Ni 2p spectra of Ni-OC_{60} and NiFe-OC_{60}.

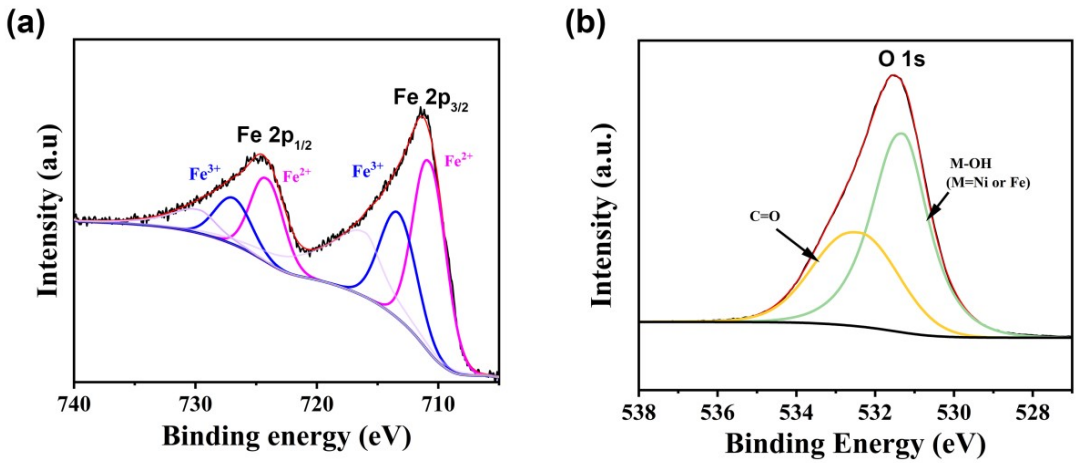

Fig. S8 (a) XPS Fe 2p spectrum of NiFe-OC_{60}, and (b) XPS O 1s spectrum of NiFe-OC_{60}.

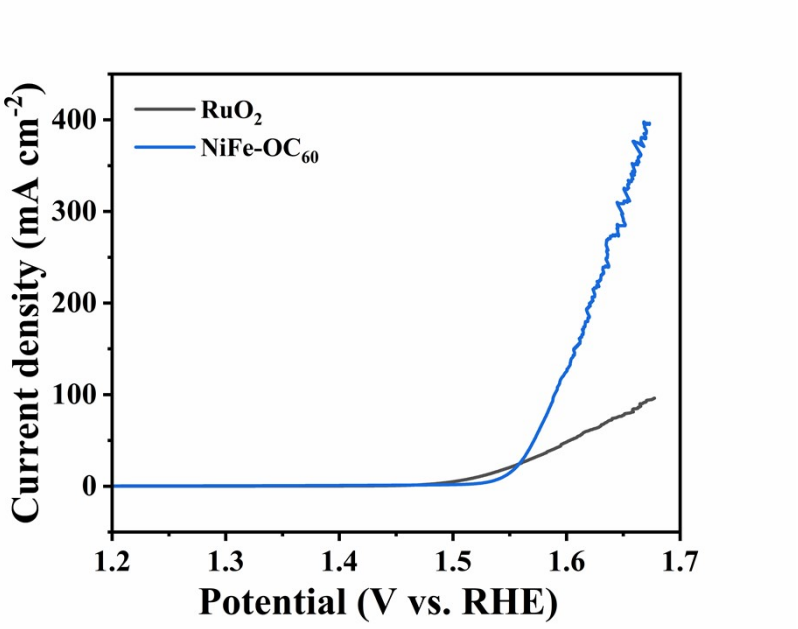

Fig. S9 LSV curves of NiFe-OC_{60} and commercial RuO_2.

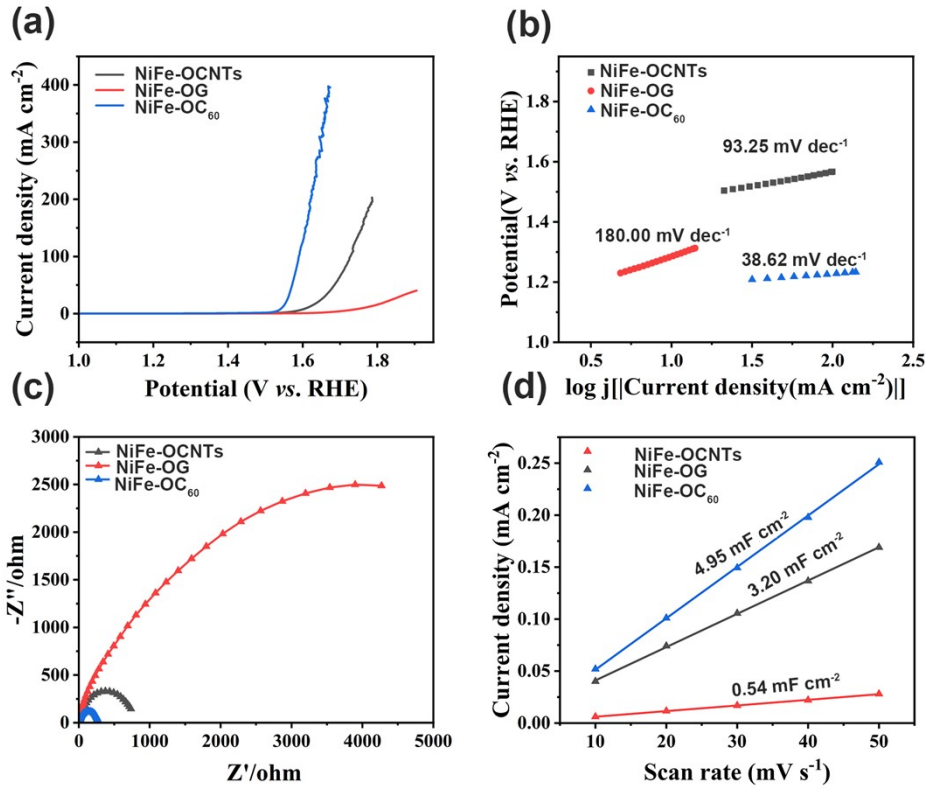

Fig. S10 Comparison of NiFe-OCNTs, NiFe-OG and NiFe-OC_{60} (a) LSV, (b) Tafel plots, (c) Nyquist plots, (d) Current density as a function of the scan rate to give the double-layer capacitance (C_{dl}).

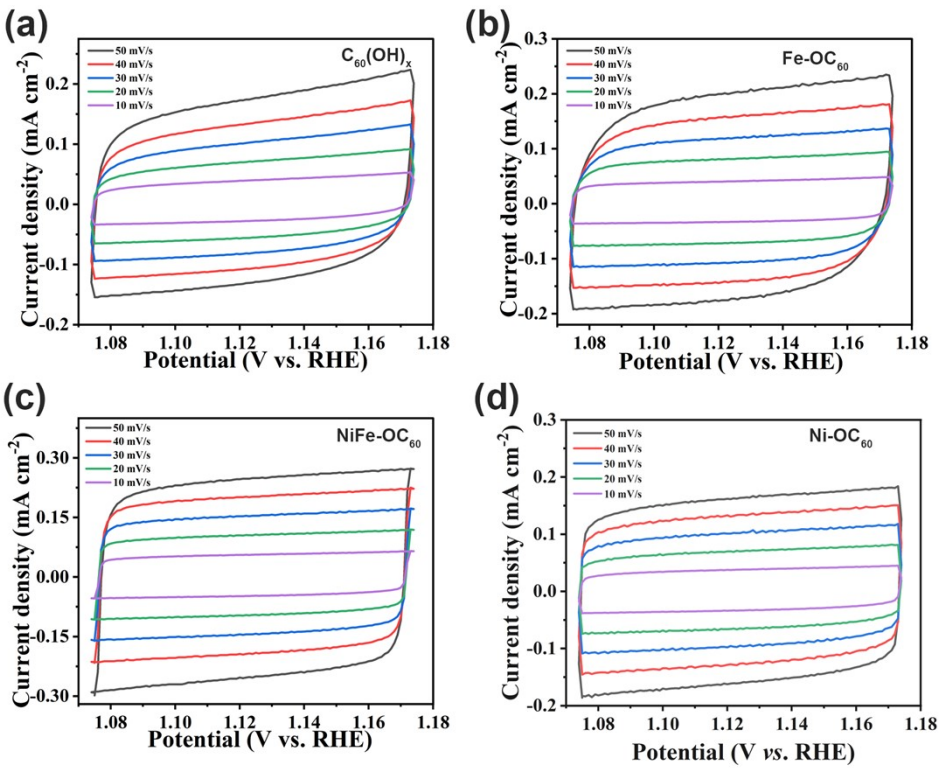

Fig. S11 CV curves of (a) $C_{60}(OH)_x$, (b) Fe-OC_{60}, (c) NiFe-OC_{60}, (d) Ni-OC_{60}.

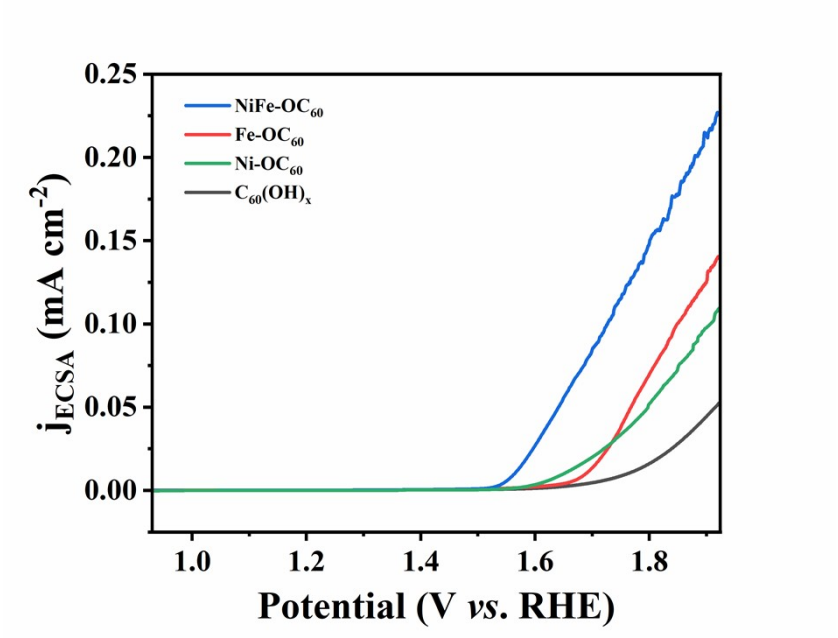

Fig. S12 ECSA-normalized LSV curves of NiFe-OC_{60}, Fe-OC_{60}, Ni-OC_{60} and $C_{60}(OH)_x$.

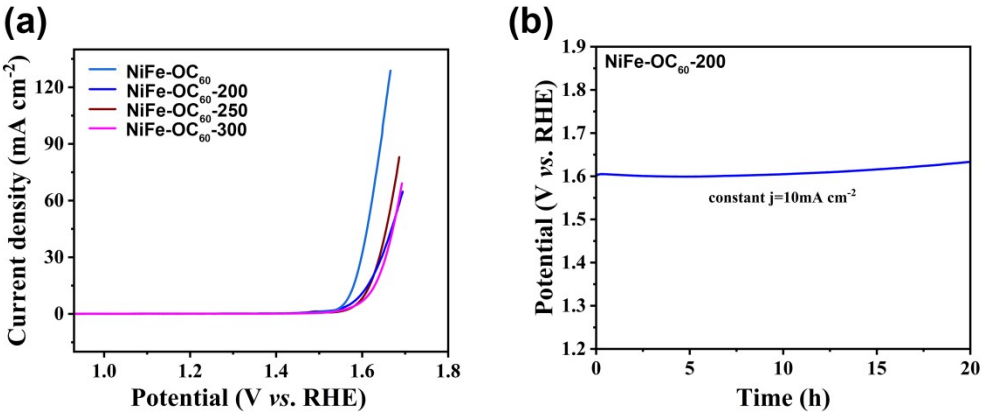

Fig. S13 (a) LSV curves of NiFe-OC_{60}, NiFe-OC_{60}-200, NiFe-OC_{60}-250 and NiFe-OC_{60}-300 samples, (b) Chronopotentiometry curve of NiFe-OC_{60}-200 measured at a fixed current density of 10 mA cm^{-2}.

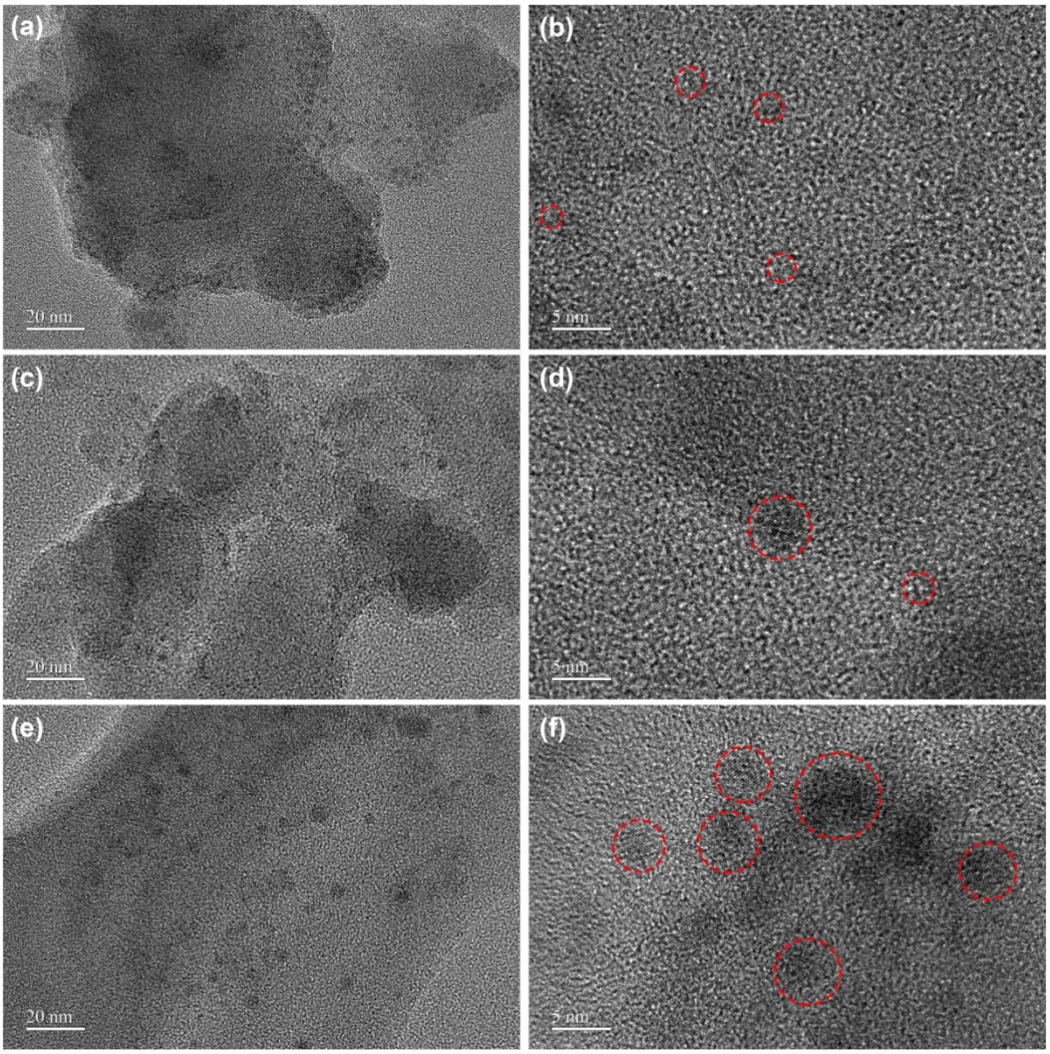

Fig. S14 TEM and HRTEM images of (a, b) NiFe-OC_{60}-200, (c, d) NiFe-OC_{60}-250, and (e, f) NiFe-OC_{60}-300 samples before OER test.

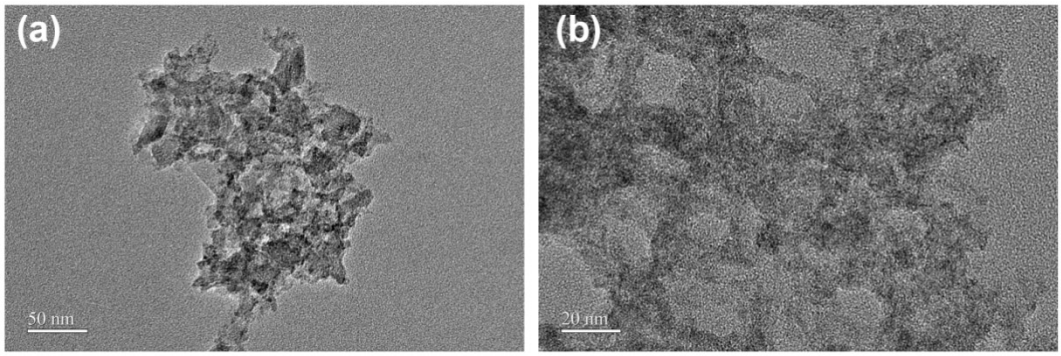

Fig. S15 (a-b) TEM images of NiFe-OC_{60} after OER stability test.

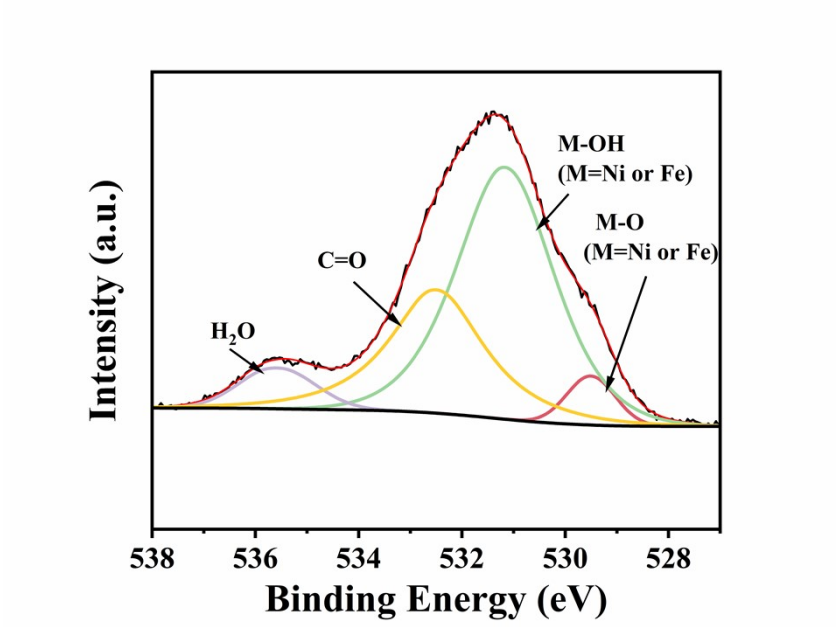

Fig. S16 High-resolution O 1s spectrum of NiFe-OC_{60} after OER stability test.

Table S1. Overpotentials and Tafel plots of NiFe-OC_{60} samples prepared with different Ni/Ni+Fe molar ratios in 1.0 M KOH.

Ni/Ni+Fe molar ratio	Overpotential (mV) @ 10 mA cm^{-2}	Current density (mA cm^{-2}) @ 1.6 V *vs.* RHE	Tafel Slop (mV dec^{-1})
0.1	334	30.29	141.15
0.3	393	5.14	202.61
0.5	383	7.26	144.02
0.7	388	5.63	154.41
0.9	314	126.11	38.62

Table S2. Comparison of NiFe-OC_{60} with some other OER electrocatalysts based on fullerene, graphene, carbon nanotube or Ni/Fe in alkaline conditions.

Catalyst	Overpotential (mV) at 10 mA cm^{-2}	Tafel slope ($mV\ dec^{-1}$)	Ref.
NiFe-OC_{60}	314	38.62	This work
Ni-OC_{60}	407.96	130.49	This work
NiFe-OCNTs	381.1	93	This work
NiFe-OG	533.5	180	This work
NFO/G	330	137.8	1
Ni-MWCNTs	320	46.16	2
p-NFNR@Ni–Co–P	272	62	3
FeNi LDH@3DG/CNs	380	77.9	4
$Ni_{0.9}Fe_{0.1}$/NC	330	45	5
FQD/CoNi-LDH	340	94	6
CeNdS/C_{60}	346	68	7
F/BCN	390	79	8
Ni-NiO@3DHPG	410	55	9
Ni–Mo_xC/NC-100	328	74	10
$NiFe_2O_4$/SWCNT	356	158	11
Fe_2N/r-GO-20	390	93	12
Ni_3N/r-GO-20	352	65	12
$NiFeO_x$	350	-	13
$NiFeO_xH_y$	348	41.5	14
NiFe LDH	310	78	15

References

1. J.-Y. Qin, S.-k. Wang, S. Zhou, T. Liu, Y.-h. Yin and J. Yang, *Adv. Energy Sustainability Res.*, 2021, **2**, 2000106.
2. S. Kang, H. Han, S. Mhin, H. R. Chae, W. R. Kim and K. M. Kim, *Appl. Surf. Sci.*, 2021, **547**, 149197.
3. Y. Feng, R. Wang, P. Dong, X. Wang, W. Feng, J. Chen, L. Cao, L. Feng, C. He and J. Huang, *ACS Appl. Mater. Interfaces*, 2021, **13**, 48949-48961.
4. Y. Li, M. Zhao, Y. Zhao, L. Song and Z. Zhang, *Part. Syst. Charact.*, 2016, **33**, 158-166.
5. X. Zhang, H. Xu, X. Li, Y. Li, T. Yang and Y. Liang, *ACS Catal.*, 2016, **6**, 580-588.
6. Y. Feng, X. Wang, J. Huang, P. Dong, J. Ji, J. Li, L. Cao, L. Feng, P. Jin and C. Wang, *Chem. Eng. J.*, 2020, **390**, 124525.
7. T. Munawar, A. Bashir, M. S. Nadeem, F. Mukhtar, S. Manzoor, M. N. Ashiq, S. A. Khan, M. Koc and F. Iqbal, *Energy Fuels*, 2023, **37**, 1370-1386.
8. M. A. Ahsan, T. He, K. Eid, A. M. Abdullah, M. L. Curry, A. Du, A. R. Puente Santiago, L. Echegoyen and J. C. Noveron, *J. Am. Chem. Soc.*, 2021, **143**, 1203-1215.
9. N. Ullah, M. Xie, L. Chen, W. Yaseen, W. Zhao, S. Yang, Y. Xu and J. Xie, *Mater. Chem. Phys.*, 2021, **261**, 124237.
10. D. Das, S. Santra and K. K. Nanda, *ACS Appl. Mater. Interfaces*, 2018, **10**, 35025-35038.
11. P. V. Shinde, R. Samal and C. S. Rout, *Trans. Tianjin Univ.*, 2022, **28**, 80-88.
12. Y. Gu, S. Chen, J. Ren, Y. A. Jia, C. Chen, S. Komarneni, D. Yang and X. Yao, *ACS Nano*, 2018, **12**, 245-253.
13. C. C. McCrory, S. Jung, J. C. Peters and T. F. Jaramillo, *J. Am. Chem. Soc*., 2013, **135**, 16977−16987.
14. D. Xu, M. B. Stevens, M. R. Cosby, S. Z. Oener, A. M. Smith, L. J. Enman, K. E. Ayers, C. B. Capuano, J. N. Renner and N. Danilovic, *ACS Catal.*, 2018, **9**, 7-15.
15. Q. Zhou, Y. Chen, G. Zhao, Y. Lin, Z. Yu, X. Xu, X. Wang, H. K. Liu, W. Sun and S. X. Dou, *ACS Catal.*, 2018, **8**, 5382-5390.